Science Journal of Energy Engineering
2025, Vol. 13, No. 2, pp. 62-70
https://doi.org/10.11648/j.sjee.20251302.13

SciencePG
Science Publishing Group

Research Article

Modeling and Simulation of a Trapezoidal Solar Collector

Mamadou Lamine Coly[1, *], Bou Counta Mbaye[2], Mamadou Seck Gueye[1], Omar Ngor Thiam[2], Joseph Sarr[1, 2]

[1]Semiconductor and Solar Energy Laboratory, Cheikh Anta Diop University, Dakar, Senegal

[2]Laboratory of Fluid Mechanics, Hydraulics and Transfer, Cheikh Anta Diop University, Dakar, Senegal

Abstract

Tunnel dryers typically employ flat double-sloped or dome-shaped collectors, which function adequately for single- rack systems but require separate components for multi- rack setups. Our innovative solution introduces an integrated trapezoidal collector that utilizes sidewalls as absorption surfaces, eliminating the need for additional units while optimizing space utilization. This study presents a comprehensive approach to designing and analyzing the trapezoidal solar collector through combined mathematical modeling and numerical simulation. Using Python's odeint library to solve thermal equations and design parameters, we identified critical interdependencies between collector components. Results demonstrate significant performance benefits: the trapezoidal design achieves 15-20% greater efficiency than conventional rectangular configurations at operational air velocities of 3.5 m/s. Under practical 900 W/m² solar irradiation, the system maintains optimal drying conditions by combining 2.5 m/s internal airflow with 4 m/s ambient wind, consistently delivering 60°C output air ideal for sensitive products like fish. The trapezoidal geometry addresses two key industry challenges - space efficiency for multi-bay systems and thermal performance optimization - by transforming sidewalls into active absorption surfaces. These findings suggest retrofitting existing tunnel dryers with trapezoidal collectors could substantially improve both energy efficiency and production throughput, particularly for temperature-sensitive food processing applications. The Python-based simulation framework further provides a valuable tool for system optimization across varying climatic and operational conditions.

Keywords

Collector, Modeling, Simulation, Solar, Thermal, Trapezoidal

1. Introduction

Air-source solar collectors are specialized devices that convert solar energy into thermal energy, primarily for air heating applications in drying processes. They come in several configurations tailored to specific operational requirements: flat-plate collectors [1, 2], tube collectors [3], and parabolic trough collectors [4]. An emerging variant incorporates geothermal Phase Change Materials (PCM) in flat-plate designs [5].

Extensive research has focused on the modeling, design, and fabrication of these collectors, with particular attention to material selection and geometric optimization to enhance both solar absorption and airflow characteristics. Notable cont*ributions include* Nourreddine Nouah et al.'s work on parabolic trough solar collectors, which demonstrated sig-

*Corresponding author: mamadouatiamine@gmail.com (Mamadou Lamine Coly)

Received: 4 May 2025; **Accepted:** 20 May 2025; **Published:** 19 June 2025

nificant improvements in energy capture efficiency. Ohannes P. et al. developed predictive models for temperature and airflow distribution in a mixed-mode solar drying system. CFD simulations were performed at different airflow velocities (ranging from 0.5 m/s to 2 m/s) and various preheater temperatures, revealing operational temperatures between 59.7 ℃ and 70.5 ℃. These models were solved using finite element methods [6, 7].

In tunnel dryers, flat plate collectors are used to supply heated air to drying chambers [8]. Conventional designs predominantly employ double-slope or dome-type flat plate collectors, with variations depending on glazing materials. These configurations are generally suitable for single-rack tunnel systems. However, multi-rack installations often require physical separation between the collector and drying chamber. To address this limitation and create an integrated unit, we utilize a trapezoidal collector configuration with the side walls functioning as the primary absorption surface.

The trapezoidal geometry offers distinct advantages by increasing solar exposure area, thereby enhancing energy conversion efficiency. To fully optimize system performance, comprehensive modeling of thermal behavior under varying environmental conditions remains essential.

2. Theoretical Study

2.1. Collector Description

The absorber is a trapezoidal-shaped flat-plate collector, comprising a horizontal absorbing plate flanked by two vertical side plates. The upper surface is glazed with a transparent window. Airflow is regulated by intake fans.

The system operates as follows: Fans force air into the collector, where it is heated through thermal transfer across the absorber walls before exiting as thermally charged airflow.

The thermal modeling approach involves:

(1) Establishing energy balances for all collector components and the heat transfer fluid.

(2) Implementing a top-down analysis (as illustrated in the figure below).

(3) Applying the energy conservation equation to account for both convective and radiative heat transfer mechanisms.

The governing energy balance equation (1) is expressed as [9]:

$$m_i C_{Pi}\left(\frac{\partial T_i}{\partial t}+\overrightarrow{V_I grad T_i}\right)=\sum h_{xij}\, S_{ij}(T_j - T_i)+\sigma_i \quad (1)$$

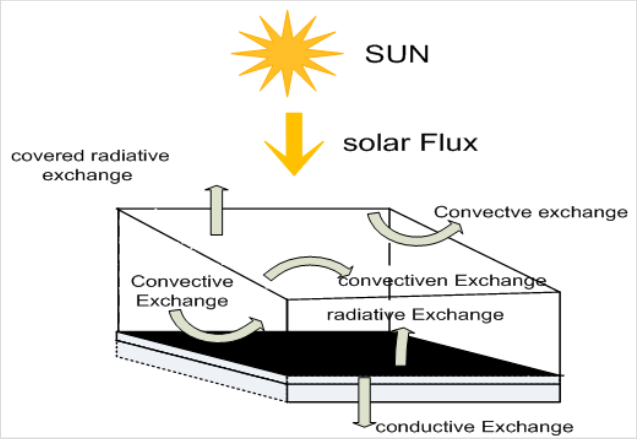

Figure 1. Phenomena heat exchanges in the absorber.

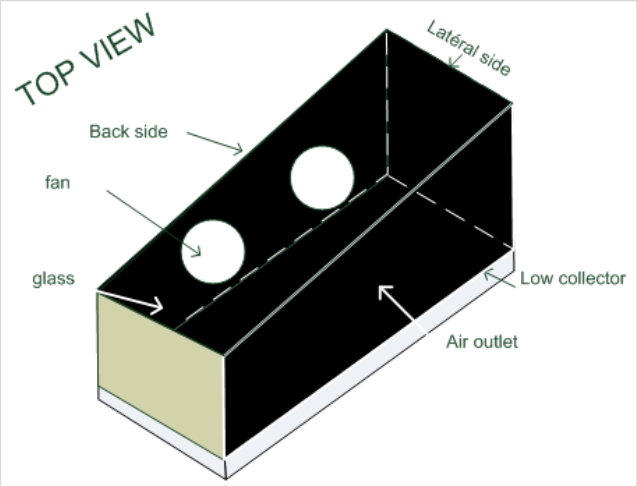

Figure 2. View inside the collector.

2.2. Solar Flux

This is the irradiance received by a wall or element during a given period. This flux is expressed in W/m ²and is defined as follows [10]:

At the coverage level:

1. solar flux on the surface of the glass:

$$\varphi_{sol} = \alpha_c S_c G \quad (2)$$

2. solar flux inside the glass:

$$\varphi_{sol} = \alpha_i \varepsilon_i S_i G \quad (3)$$

2.3. Radiative Flux

These radiative exchanges occur between the various elements inside the dryer, as well as between the cover and the vaulted celestial. Under appropriate assumptions, they can be expressed as follows [11]:

$$\phi_r = h_{r,1-2}(T_1^4 - T_2^4) \quad (4)$$

1. Radiation coefficient between the cover and the vaulted celestial

We *adopt the* relationship proposed in equation (5) [12]:

$$h_{r,c-a} = \sigma.\varepsilon_c\left(\frac{1-\cos\beta}{2}\right) \quad (5)$$

2. Temperature of the vaulted celestial

$$T_v = 0.0552T_{ae} \quad (6)$$

With Tae the ambient air temperature

3. Radiation coefficient between two walls 1 and 2 [13]

$$h_{r,1-2} = \frac{\sigma}{\frac{1-\varepsilon_1}{\varepsilon_1} + \frac{1}{F_{1-2}} + \frac{1-\varepsilon_2}{\varepsilon_2}\left(\frac{S_1}{S_2}\right)} \quad (7)$$

With $F_{1\text{-}2}$ form factor

2.4. Convective Flow

It describes the heat exchanges between a fluid and a wall, it is defined by [14]:

$$\phi_{c,1-2} = h_{c,1-2}S(T_1 - T_2) \quad (8)$$

1. The convection coefficient between the cover and the outside air is calculated by the following Hottel and Woertz relationship [15]:

$$h_{c,c-a} = 5.7 + 3.8v_{vent} \quad (9)$$

With v_{vent}: average wind speed

2. Convection coefficient between the drying air and the walls [16].

This coefficient is determined from the Nusselt number. We will determine the exchange coefficient for each wall of a trapezoidal geometry crossed by air.

$$h_c = \frac{\lambda N_u}{D_n} \quad (10)$$

D_n: a characteristic length for the walls of the dryer.

N_U: the Nusselt number [17]:

$$N_u = 0.019R_e^{0.8}P_r^{\frac{1}{3}} \quad (11)$$

Re is the Reynolds number defined by [18]:

$$R_e = \frac{VD_n}{\nu} \quad (12)$$

With V: air speed

$$\nu = 10^{-5}(0.006T_a + 1.7176) \quad (13)$$

and the number of Prandtl:

Pr = 0.73 for air

To model our collector, we will make some simplifying assumptions.

Hypotheses:

(1) The cover is opaque to IR radiation.

(2) The flow is one-dimensional along the longitudinal axis.

(3) The temperature of the cover on both sides is uniform.

(4) The temperature fields T_c of the cover, T_P of the absorber and T_{pl} of the side wall are uniform.

(5) The physical properties of the materials making up the dryer are constant.

(6) The ambient temperature is the same around the collector.

(7) The fluid flow is laminar.

(8) The radiation between the absorbing and side walls is neglected.

2.5. Presentation of the Mathematical Model of the Collector

1. At the cover level

$$\frac{dT_c}{dt} = \frac{\alpha_v G + h_{c,c-f}(T_f - T_c) + h_{r,pr-c}(T_p^4 - T_c^4) + h_{c,c-a}(T_a - T_c) + h_{r,c-v}(T_v^4 - T_c^4) + h_{r,pl-c}(T_{pl}^4 - T_c^4)}{\rho_c e_c c_c} \quad (14)$$

$h_{r,pr-c}$: radiation transfer coefficient between absorbent wall and cover.

$h_{c,c-a}$: convection transfer coefficient between the cover and ambient air.

$h_{c,c-f}$: convection transfer coefficient between the cover and the heat transfer fluid.

$h_{r,c-v}$: radiation transfer coefficient between the cover and the vaulted celestial.

$h_{r,pl-c}$: radiation transfer coefficient between the side wall and the cover.

2. At the level of the absorbent wall

$$\frac{dT_p}{dt} = \frac{\alpha_p \tau_v G + h_{c,p-f}(T_f - T_p) + h_{r,p-c}(T_p^4 - T_c^4) + h_{r,p-pl}(T_{pl}^4 - T_p^4)}{\rho_p e_p c_p} \quad (15)$$

$h_{c,p-f}$: convection transfer coefficient between the absorbent wall and the fluid.

$h_{r,p-c}$: radiation transfer coefficient between wall and cover.

$h_{r,pr-pl}$: radiation transfer coefficient between absorbing wall and side wall.

3. At the level of the heat transfer fluid

$$\frac{\mathrm{dT_f}}{\mathrm{dx}} = \frac{h_{c,c-f}S_c(T_c - T_f) + h_{c,p-f}S_p(T_p - T_f) + h_{c,pl-f}S_{pl}(T_{pl} - T_f)}{D_m \Delta x c_f} \quad (16)$$

$h_{c,c-f}$: convection transfer coefficient between the cover and the fluid.

$h_{c,p-f}$: convection transfer coefficient between the absorbent wall and the fluid.

$h_{c,pl-f}$: convection transfer coefficient between the side wall and the fluid.

4. At the side wall level

$$\frac{dT_{pl}}{dt} = \frac{\alpha_{pl}\tau_v G + h_{c,pl-f}(T_f - T_{pl}) + h_{r,pl-c}(T_c^4 - T_{pl}^4) + h_{r,p-pl}(T_p^4 - T_{pl}^4)}{\rho_{pl} e_{pl} c_{pl}} \quad (17)$$

$h_{r,p-Pl}$: radiation transfer coefficient between the side wall and the cover.

$h_{c,pl-f}$: convection transfer coefficient between the side wall and the fluid.

$h_{r,pl-c}$: radiation transfer coefficient between the side wall and the cover.

3. Results and Discussion

The system of equations was solved in Python using the ODEINT library. The calculations were performed for three drying air velocities (2.5, 4.5, and 6 m/s) and three constant solar flux values (500, 700, and 900 W/m²), representing the maximum solar flux density. We specifically analyzed wind speed effects at a maximum flux of 900 W/m² and an air velocity of 2.5 m/s. The presented results focus on: (1) wind speed influence, (2) solar flux influence, and (3) spatio-temporal temperature distributions of the collector components.

3.1. Influence of Wind Speed

Analysis of the results (Figure 3) demonstrates that wind speed critically influences the solar collector's thermal evolution.

All wall temperatures show progressive increases before stabilizing after three hours.

Figure 3a (glass cover) reveals this component's exceptional sensitivity to wind variations, displaying a marked temperature decrease caused by enhanced convective heat transfer from direct environmental exposure.

Figure 3b (heat transfer fluid) and 3c (absorber) exhibit more moderate thermal responses, reflecting greater thermal inertia from the fluid's energy storage capacity and radiative absorption effects.

Figure 3d (sidewall) presents intermediate behavior—less affected than the glass cover but more responsive than the absorber—consistent with its secondary role in thermal transfer processes.

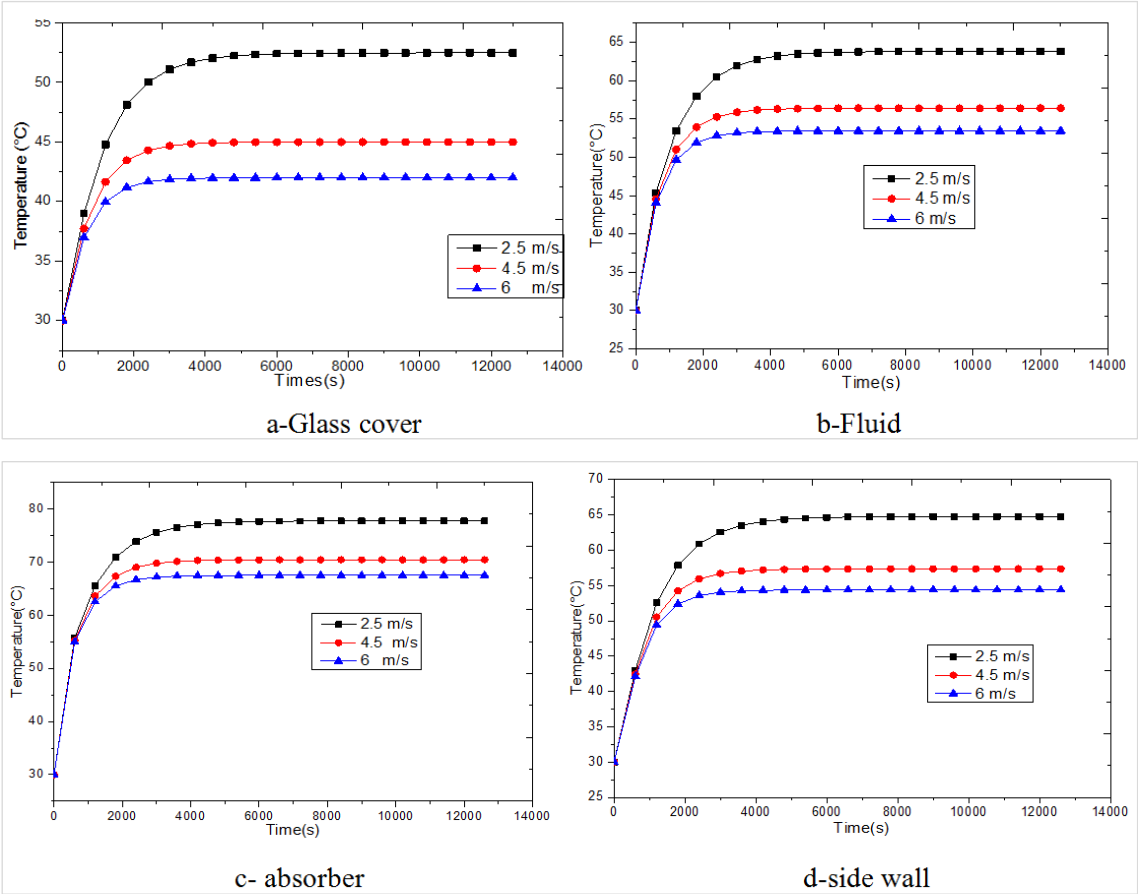

Figure 3. *Variation de la température du capteur en fonction du temps selon la vitesse d'entrée de l'air.*

These results clearly establish that wind effects are highly component-dependent, varying by material properties and spatial position. The glass cover emerges as the most critical element, experiencing the most significant convective losses.

Consequently, targeted improvements in cover insulation or aerodynamic design could substantially boost collector efficiency during windy operation.

3.2. Influence of Irradiance

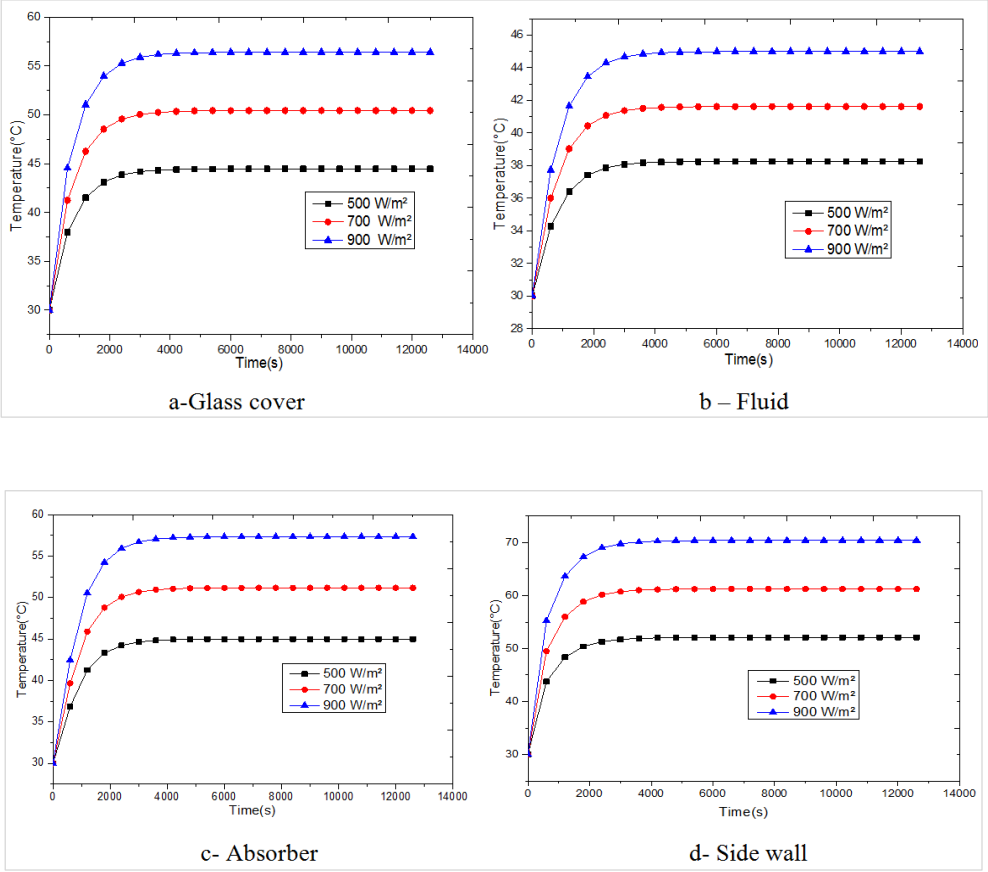

Figure 4. *Temperature variation as a function of time for different irradiances, for V=3.5m/s.*

Figure 4 demonstrates the effect of solar flux variation on temperature evolution across collector walls at constant air velocity. All wall temperatures show progressive increases before stabilizing after three hours of solar exposure. As expected, higher solar radiation intensities produce greater temperature increases, as evidenced by the curve profiles.

The glass cover (Figure 4a), heat transfer fluid (Figure 4b), absorber (Figure 4c), and side wall (Figure 4d) each exhibit distinct temperature responses to solar flux density. Maximum temperatures reach 44 ℃, 56 ℃, 70 ℃, and 57 ℃ for the cover, fluid, absorber, and side wall respectively at 900 W/m ² flux density, compared to minimum values of 38 ℃, 44 ℃, 52 ℃, and 44 ℃ at 500 W/m ².

This thermal behavior stems from the material's absorptive properties and surface characteristics. Functioning as a black body, the absorber accumulates more thermal energy than other components, resulting in significantly higher temperatures.

3.3. Influence of Air Speed

Figure 5 shows the influence of varying air speed on the temperature evolution of the different collector walls for a constant irradiance. Varying air speed has a significant impact on the temperature evolution of the different walls of the solar collector. Higher air speed increases convective heat transfer, which cools the collector walls more quickly (Figure 5b, c and d). Lower air speed decreases convective heat transfer, allowing the walls to retain more heat. Increasing air speed increases convective heat transfer at the cover (Figure 5a), thus increasing the cover temperature.

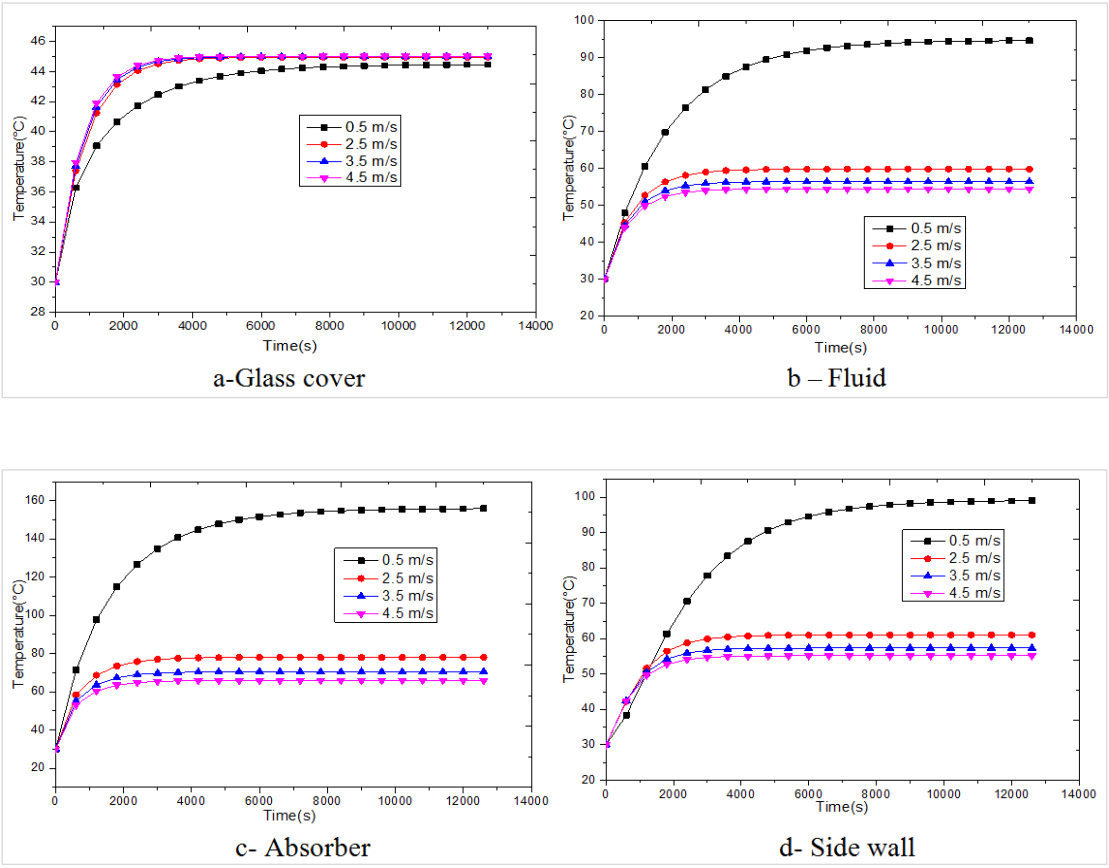

Figure 5. *Temperature variation over time for different speeds.*

3.4. Influence of the Color of the Side Wall

Figure 6 shows the influence of the sidewall color on the temperature evolution of the collector for constant irradiance. Black color presents higher temperatures, because a black sidewall can redistribute the absorbed heat to the other walls of the collector, thus increasing the overall temperature of the system.

On the other hand, light colors reflect a large portion of solar energy. This can reduce the temperature increase of the side walls. This temperature difference is noted on the side wall (Figure 6d), which directly absorbs sunlight. Therefore, black color increases the temperature of this absorbing wall.

For the cover (Figure 6a), it is less directly affected by the color of the side walls, but it feels the indirect effects via convection heat transfer.

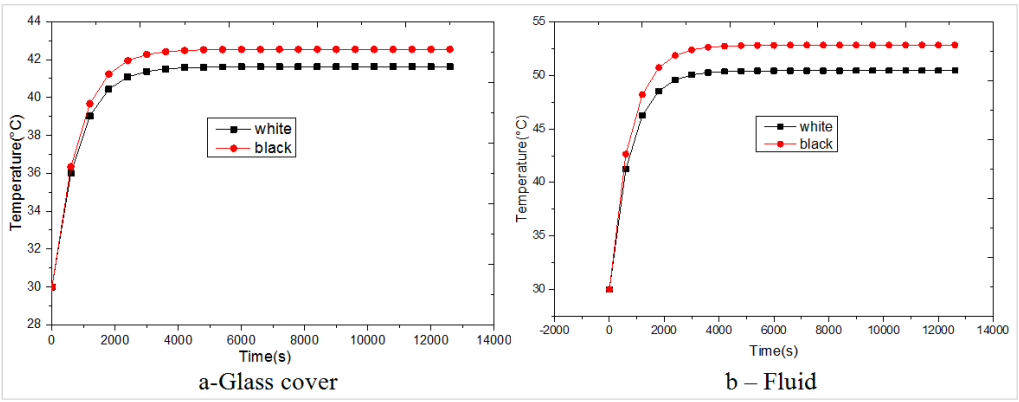

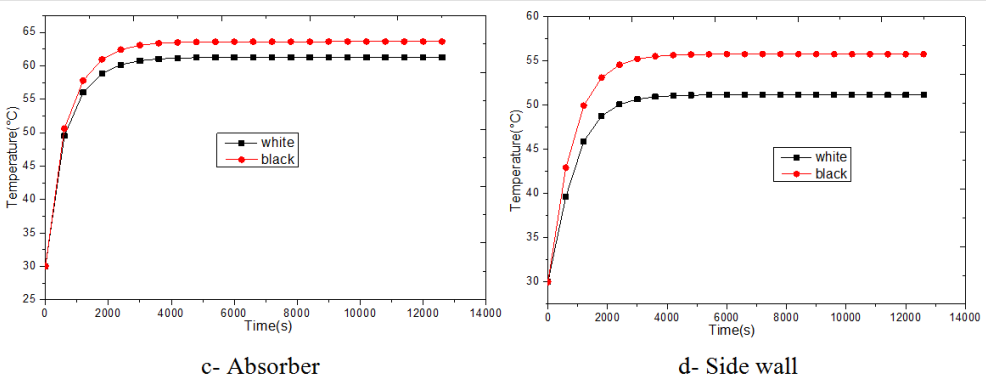

Figure 6. *Temperature variation by changing the color of the wall faces.*

3.5. Influence of the Variation Resulting of Height of the Lateral Face

Figure 7 illustrates the effect of rear face height on the temperature evolution across the collector walls under constant irradiance and speed conditions.

A taller rear face enhances internal air circulation within the collector, improving convective heat transfer (Figure 7d). At the cover (Figure 7a), as the absorber-cover distance decreases, convective heat transfer becomes more pronounced, slightly raising the cover's temperature. Conversely, for the heat transfer fluid (Figure 7a), a fixed irradiance results in lower temperatures as the absorber-cover gap narrows.

At a speed of V = 2.5 m/s, the rear face height influences heat distribution across the collector walls. A greater height increases the absorber's capture surface, leading to higher temperatures, while a reduced height diminishes the capture surface, in lower temperatures.

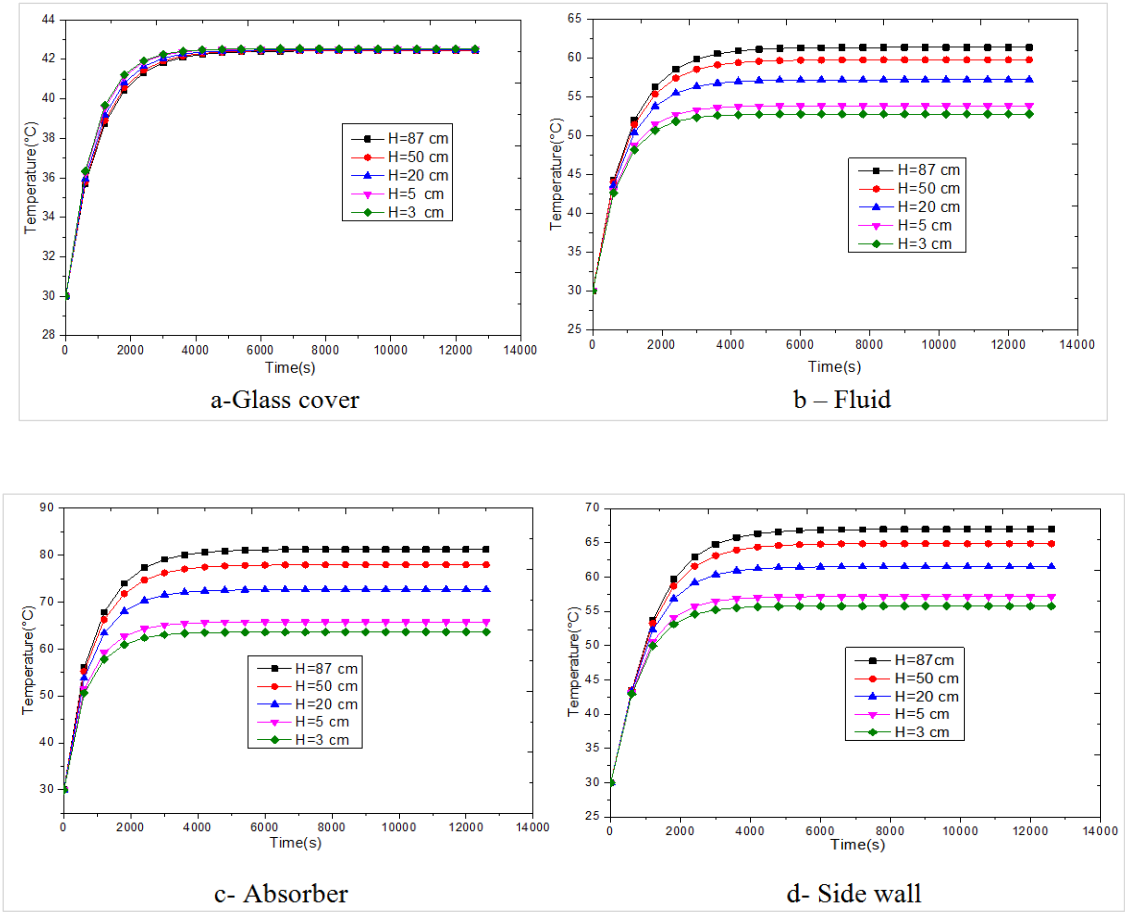

Figure 7. *Temperature variation for different rear wall heights.*

4. Conclusions

Our Python-optimized trapezoidal solar collector demonstrates superior performance for agricultural drying applications. Key operational parameters reveal that maintaining 2.5 m/s airflow at 900 W/m ²irradiance achieves optimal drying temperatures, with collector height significantly affecting efficiency. The trapezoidal design delivers 15-20% greater energy capture than rectangular counterparts at working airspeeds, while blackened interior walls further enhance performance through improved heat absorption. This optimized configuration offers food processors an immediately implementable solution that maintains consistent drying temperatures with lower energy requirements. The design's simple structural modification from conventional collectors makes it particularly suitable for industrial-scale solar drying systems operating at moderate to high airflow rates.

Abbreviations

c_p	Heat Capacity J $kg^{-1}.°C^{-1}$
G	Irradiance Wm^{-2}
M	Air Mass Flow Rate $kg.s^{-1}$
P_{th}	Thermal Power W
P_n	Fan Power W
S_b	Absorber Capture Surface m²
Sc	Trays Surface m²
T_P	Absorbent Wall Temperature°C
T_f	Fluid Temperature at the Dryer Outlet°C
Tc	Blanket Temperature°C
t	Drying Time H
T_{pl}	Wall Temperature°C
α	Absorption Coefficient
β	Tilt Angle Rad
ε	Reflection Coefficient
η_{th}	Thermal Sensor Performances
λ	Air Conductivity W $m^{-1}.K^{-1}$
ν	Kinematic Viscosity of Air $m^2.s^{-1}$
ρ	Density $kg.m^{-3}$
τ	Transmission Coefficient
σ	Stephan-Boltzmann Constant Wm^{-2} K^{-4}

Acknowledgments

This section serves to recognize contributions that do not meet authorship criteria, including technical assistance, donations, or organizational aid. Individuals or organizations should be acknowledged with their full names. The acknowledgments should be placed after the conclusion and before the references section in the manuscript.

Author Contributions

Mamadou Lamine Coly: Conceptualization, Writing – original draft

Bou Counta Mbaye: Software, Visualization

Mamadou Seck Gueye: Methodology, Validation

Omar Ngor Thiam: Methodology, Validation

Joseph Sarr: Supervision

Funding

This work is not supported by any external funding.

Data Availability Statement

The data is available from the corresponding author upon reasonable request.

Conflicts of Interest

The authors declare no conflicts of interest.

References

[1] Belghit, A., Belahmidi, M., Bennis, A., Boutaleb, BC, Benet, S. Numerical study of a solar dryer operating in forced convection. Rev. Générale Therm. 1997, 36, 837–850. https://doi.org/10.1016/S0035-3159(97)87754-9

[2] Djebli, A., Hanini, S., Badaoui, O., Haddad, B., Benhamou, A. Modeling and comparative analysis of solar drying behavior of potatoes". Renew Energy. 2020, 145, 1494-1506. https://doi.org/10.1016/j.renene.2019.07.083

[3] Iranmanesh, M., Akhijahani, HS, Jahromi, MSB. CFD modeling and evaluation the performance of a solar cabinet dryer equipped with evacuated tube solar collector and thermal storage system. Renew. Energy. 2020, 145, 1192–1213.

[4] Nourreddine Nouah *, Nabil Djennaoui and Tinhinane Hassani: Modeling of a cylindrical-parabolic solar collector. Renewable Energy Review 2014, 17 (4), 559 – 567. https://doi.org/10.54966/jreen.v17i4.469

[5] Ananno, AA, Masud, MH, Dabnichki, P., Ahmed, A. Design and numerical analysis of a hybrid geothermal PCM flat plate solar collector dryer for developing countries. Ground. Energy 2020, 196, 270–286. https://doi.org/10.1016/j.solener.2019.11.069

[6] KUMAR, L., PRAKASH, O. & PANDEY, VK Numerical modeling of a hybrid greenhouse solar dryer with single-pass solar air heater for bitter gourd flakes drying: a finite element analysis Sādhanā. 2024, 49, 250. https://doi.org/10.1007/s12046-024-02583-z

[7] Abubakar S, Anafi F, Kaisan M, Narayan S, Umar S, Umar U. Comparative analyzes of experimental and simulated performance of a mixed-mode solar dryer. Proceedings of the Institution of Mechanical Engineers, Part C: Journal of Mechanical Engineering Science. 2020, 234(7), 1393-1402. https://doi.org/10.1177/0954406219893394

[8] Armand Noël Ngueche Chedop 1, Noël Djongyang 1, Zaatri Abdelouahab: Modeling and comparative study of flat and tube solar collectors in the Sudano-Sahelian regions of Cameroon. Sciences & Technologie. 2018, 47, 37-44.

[9] Incropera, F. P., DeWitt, D. P., Bergman, T. L., & Lavine, A. S. *Fundamentals of Heat and Mass Transfer* (2017), (8th ed.). Wiley.

[10] ASHRAE. *ASHRAE Handbook—Fundamentals*. American Society of Heating, Refrigerating and Air-Conditioning Engineers. *Climatic Design Information* 2021, 14.1–14.XX. ISBN: 978-1-947192-98-2 (édition SI) / 978-1-947192-97-5 (édition I-P). Chapitre 14.

[11] Modest, M. F. *Radiative heat transfer* (3rd ed.). Academic Press. (2013), ISBN: 978-0-12-386944-9 (hardcover) / 978-0-12-386990-6 (eBook), https://doi.org/10.1016/B978-0-12-386944-9.00001-8

[12] Slim, R.. Modeling and design of a solar greenhouse assisted by heat pumps for drying sewage treatment plant sludge, Doctoral thesis, Ecole des Mines de Paris, Paris, 2007. 145.

[13] Pallet, D., Fournier, M., Themelin, A. Modeling, identification and simulation of a solar wood dryer. Rev. Phys. Appliquée.1987, 22, 1399–1409. https://doi.org/10.1051/rphysap:01987002201101399000

[14] Eshetu Getahun a, b, c, Mulugeta A. Delelec*, Nigus Gabbiyec, Solomon W. Fantac, Petros Demissieb 3 Maarten Vanierschot: Importance of integrated CFD and product quality modeling of solar dryers for fruits 2 and vegetables: A review. Solar Energy 2021, 220, 88-110, https://doi.org/10.1016/j.solener.2021.03.049

[15] Benaouda, N.-E., Belhamel, M. Modeling of a solar tobacco drying system in Algeria, in: JITH 2007. ENSTIMAC, p. 5p.

[16] Motahayyer, M., Arabhosseini, A., Samimi-Akhijahani, H. Numerical analysis of thermal performance of a solar dryer and validated with experimental and thermo-graphical data. Ground. Energy. 2019, 193, 692–705. https://doi.org/10.1016/j.solener.2019.10.001

[17] Vásquez, J., Reyes, A., Pailahueque, N. Modeling, simulation and experimental validation of a solar dryer for agro-products with thermal energy storage system. Renew. Energy, 2019, 139, 1375–1390. https://doi.org/10.1016/j.renene.2019.02.085

[18] KUMAR, Lalan and PRAKASH, Om. Optimal simulation approach for tomato flakes drying in hybrid solar dryer. Energy Sources, Part A: Recovery, Utilization, and Environmental Effects, 2024, 46, 1, 5867-5887.

Research Field

Mamadou Lamine Coly: Solar energy systems, Thermal engineering, drying of food products, Heat transfer, Computational fluid dynamics.

Bou Counta Mbaye: Energy efficiency, Solar thermal collectors, Numerical modeling, Sustainable engineering, Fluid mechanics.

Mamadou Seck Gueye: Solar energy systems, Thermal engineering, drying, Heat transfer, Dying, Energy sustainability.

Omar Ngor Thiam: Energy efficiency, Solar thermal collectors, Numerical modeling, Sustainable engineering, Fluid mechanics.

Joseph Sarr: Solar energy systems, Thermal engineering, drying, Heat transfer, Energy sustainability.